Proceedings of the 20th International Conference on Soil Mechanics and Geotechnical Engineering– Rahman and Jaksa (Eds)

Effect of geocell inclusion on railway ballast stability

Effet de l'inclusion de Geocell sur la stabilité du ballast ferroviaire

Rufaida Zikria & Shah Neyamat Ullah
School of Engineering and Technology, Central Queensland University, Australia

ABSTRACT: Railway foundations need a relatively strong ballast to reduce track settlement induced due to heavy wheel loads from trains. Geocell inclusions have shown to improve subgrade conditions by providing lateral confinement to the ballast. In this study, a numerical model of a plate load test followed by a railway foundation model was developed using a commercially available finite element software ABAQUS. After successful validation of the plate load numerical model with existing finite element (FE) model data and experimental data, the scope of the study was extended in developing a railway model with realistic railroad conditions. Models with and without geocell inclusion were simulated, and results were obtained in terms of vertical settlement and stresses. To model the elastoplastic behavior of the ballast, the Drucker Prager yield criterion was used, while the diamond shaped geocells were modelled as a linear elastic material. To mimic the real-life train wheel load effects, cyclic loading up to 80,000 cycles were simulated. The cyclic load was applied in a stress-controlled manner over a frequency of 16 Hz using a haversine amplitude function corresponding to the speed of fast and heavy haul trains reaching a velocity of 120 km/hr. The results showed a substantial performance improvement with geocell reinforcement. The vertical deformation reduced by 12% at the track level and 45% at the subgrade interface after 80,000 cycles due to the geocell reinforcement. There was a substantial reduction in vertical stresses up to a maximum of 40% at the track level. The geocell reinforcement model also shows a more uniform stress distribution compared to a rapidly fluctuating stress response for the unreinforced model.

RÉSUMÉ : Les fondations ferroviaires ont besoin d'un ballast relativement solide pour réduire le tassement de la voie induit par les lourdes charges sur les roues des trains. Il a été démontré que les inclusions de géocellules améliorent les conditions de fondation en fournissant un confinement latéral au ballast. Dans cette étude, un modèle numérique d'un essai de charge de plaque suivi d'un modèle de fondation ferroviaire a été développé à l'aide d'un logiciel d'éléments finis disponible dans le commerce ABAQUS. Après une validation réussie du modèle numérique de charge de plaque avec des données de modèle d'éléments finis (EF) existantes et des données expérimentales, la portée de l'étude a été étendue en développant un modèle ferroviaire avec des conditions ferroviaires réalistes. Des modèles avec et sans inclusion de géocellules ont été simulés et des résultats ont été obtenus en termes de tassement vertical et de contraintes. Pour modéliser le comportement élastoplastique du ballast, le critère d'élasticité de Drucker Prager a été utilisé, tandis que les géocellules en forme de losange ont été modélisées comme un matériau élastique linéaire. Pour imiter les effets réels de la charge sur les roues du train, des charges cycliques allant jusqu'à 80 000 cycles ont été simulées. La charge cyclique a été appliquée de manière contrôlée en contrainte sur une fréquence de 16 Hz en utilisant une fonction d'amplitude sinusoïdale correspondant à la vitesse des trains de transport rapides et lourds atteignant une vitesse de 120 km/h. Les résultats ont montré une amélioration substantielle des performances avec le renforcement des géocellules. La déformation verticale a été réduite de 12 % au niveau de la voie et de 45 % à l'interface du sol de fondation après 80 000 cycles grâce au renforcement des géocellules. Il y a eu une réduction substantielle des contraintes verticales jusqu'à un maximum de 40 % au niveau de la voie. Le modèle de renforcement des géocellules montre également une distribution des contraintes plus uniforme par rapport à une réponse aux contraintes fluctuant rapidement pour le modèle non renforcé.

KEYWORDS: Geocells, finite element analysis, railway, ballast, soil, transportation

1 INTRODUCTION

Railways form the world's largest catering network for fast and reliable public and freight transport. There is a high demand in Australia and around the world to make future railways faster with an increase in freight capacity (Indraratna et al. 2017). However, increase in repeated dynamic loads may cause frequent maintenance issues and progressive deterioration of the railway substructure (Figure 1). This in turn may result in excessive rail track settlement and possible derailment especially when the subgrade soil is of poor quality (Li & Hao, 2015; Satyal et al. 2018).

Railway ballast performs many key functions for smooth railway operation, including uniform distribution of oncoming stresses, dampening the wheel loading impacts, reducing vibrations, minimising long term settlements, and providing a competent base (Selig & Waters, 1994). These functions of the

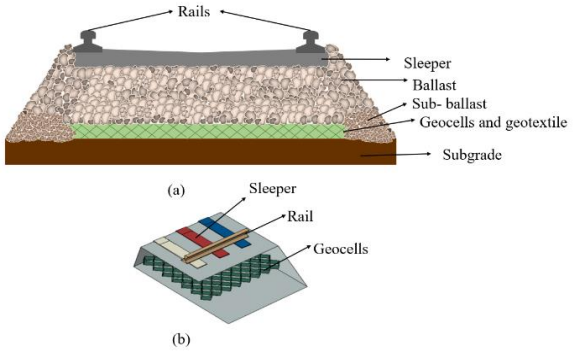

Figure 1. (a) Typical railway ballast substructure with geocell reinforcement and (b) placement of geocell

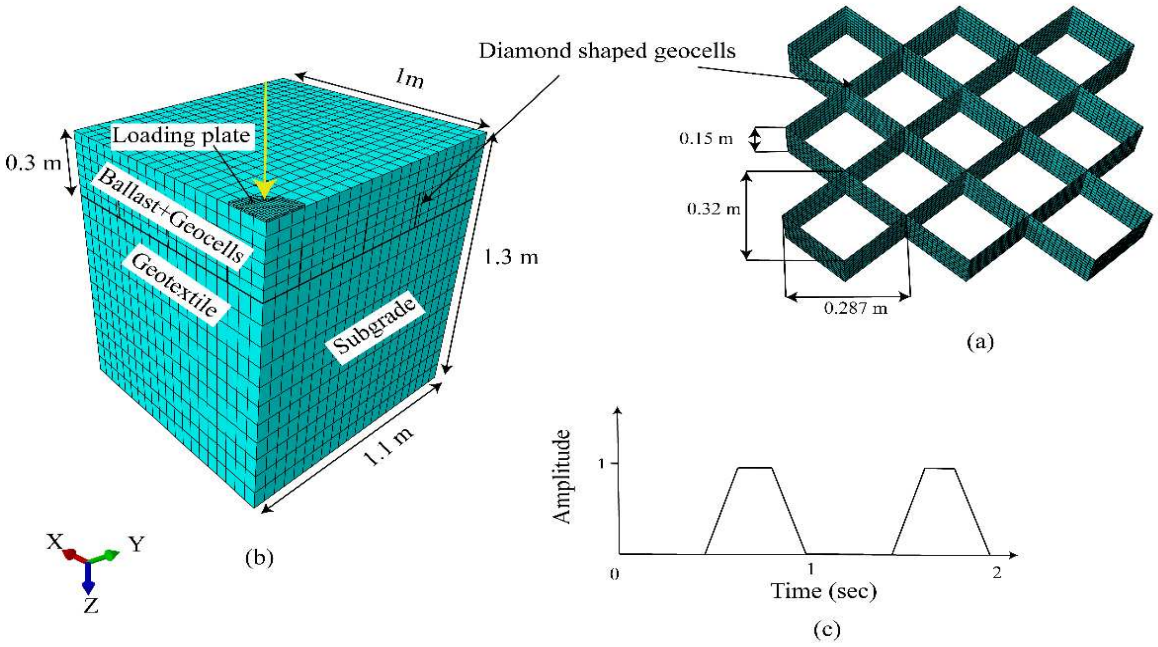

Figure 2. Details of finite element model of the cyclic plate model test: (a) diamond-shaped geocells used in analysis and (b) model geometry of the plate loading test (c) haversine loading pattern used in experiment and finite element analysis.

ballast layer may be compromised when the subgrade soil consists of soft clay due to excessive settlement of the clay layer inducing overall track instability (see Bergado & Rajagopal, 2015; Biswas et al. 2015; Chaney et al. 2000; S. Dash & Shivadas, 2012).

Several ground improvement techniques such as vacuum consolidation (T.K Dam et al. 2006), use of prefabricated vertical drains with surcharge loading (Indraratna, 2008) as well as soil reinforcement with geogrids or geocells are possible alternatives (Lackenby et al. 2007; Nimbalkeret et al. 2014; Satyal et al. 2018).

Geocells are interconnected three dimensional cells usually made of high-density polyethylene (HDPE), polyester or any other polymer material. Geocells provide a three-dimensional confinement to the soil layer they are installed in and inhibits potential lateral soil movement i.e., lateral spreading. In railway structures, they are mostly installed in the sub-ballast or capping layer sufficiently far from the wheel load to allow sufficient space for railway machinery to operate during ballast cleanup and track maintenance, as well as to prevent structural damage to the geocell walls. Apart from providing confinement, geocell reinforced soil layer acts as a mattress reducing vertical stresses transferred to the weak subgrade. Several studies have shown that geocells can significantly improve the ground conditions by reducing subgrade deformation as well as stresses (Hegde & Sitharam, 2013; Rajagopal et al. 1999; Dash & Shivadas, 2012; Hegde, 2017; Mhaiskar & Mandal, 1996). While most previous research idealise the geocell-soil interaction as a two-dimensional problem, such idealisation may result in inaccurate assessment of stresses in soil (Garcia & Avesani Neto, 2021; Punetha et al. 2020). Limited research has been carried out to investigate the effect of the geocell reinforcement in the railway substructure. Biabani et al. (2015) performed model testing using a specialised testing ring suggesting geocells can reduce lateral spreading of the railway ballast. Satyal et al. (2018) performed model experiments as well as finite element (FE) modelling under repeated wheel load conditions up to 100,000 cycles and showed that under certain conditions geocells may reduce the track settlement by as much as 90%.

In this paper, a three-dimensional finite element (FE) analysis was performed for a geocell reinforced railway structure using the commercially available software ABAQUS/Explicit (ABAQUS, 2019). The FE model was verified using model test data available in the literature and extended to consider repeated train wheel loading up to 80,000 cycles. The track settlement, subgrade stresses and deformation at key locations were monitored.

2 FINITE ELEMENT ANALYSIS

A three-dimensional FE model for a cyclic plate load test conducted at the Kansas State University (see Satyal et al. 2018) is developed first (Figure 2). The validated model is then extended modelling a typical Australian railway structure where the subgrade consists of soft clay. A brief description of the experiment followed by FE modelling details are provided below.

2.1 *Cyclic plate load model experiment*

The experiments were conducted in a strongbox of dimensions 2 m wide, 2.2 m long and 2 m depth filled with a Kaolin sand mixture was used as subgrade underlying a standard uniformly graded track ballast which followed the AREMA 4A (American Railway Engineering and Maintenance) specifications (mean particle size D_{50} = 32 mm, maximum and minimum density of 1525 and 1340 kg/m^3, respectively). A loading plate attached to a hydraulic actuator was used to provide cyclic loading at a1 Hz frequency with 1000 cycles for each loading step forming a haversine waveform (Figure 2). For the reinforced test, a geotextile was placed at the ballast subgrade interface followed by placement of commercially available polyethylene polymer geocells (Presto Geosystem; Geoweb GW30V). The pocket size of the cells was 287 mm by 320 mm with a depth of 150 mm. The geocells were placed on top of the prepared subgrade and compacted with the ballast particles to their maximum density with a handheld pneumatic tamper.

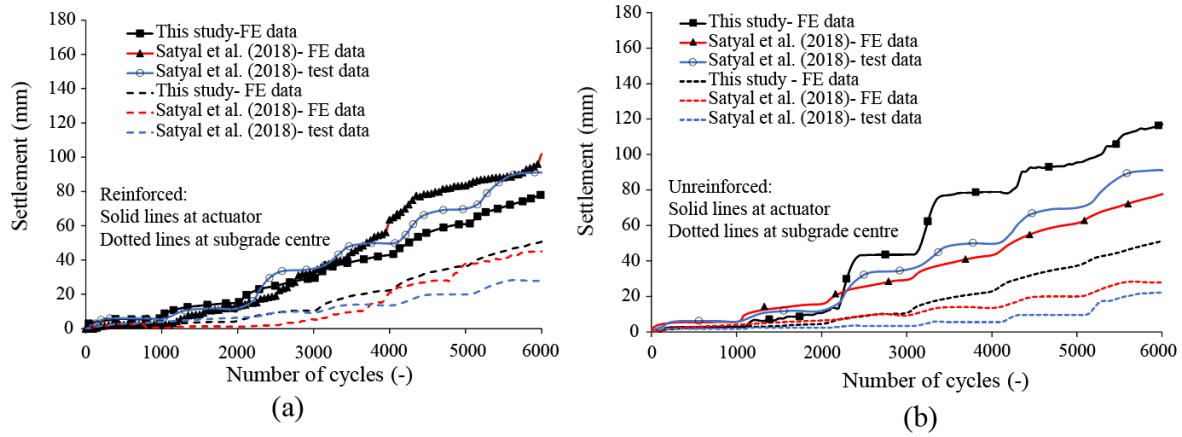

Figure 3. Settlement comparison with experimental and FE data of Satyal et al. (2018), (a) Geocell reinforced model and (b) Unreinforced model

2.2 *Cyclic plate load ABAQUS FE model*

FE model is shown in Figure 2. The ballast height was 0.3 m and modelled as a non-associative elastic-plastic material obeying the 3D linear Drucker-Prager yield criterion. The friction angle β was set at 45° with a dilation angle ψ of 10°. The shear strength properties and elastic modulus of ballast were obtained from the literature (see Satyal et al. 2018). The soft subgrade was modelled as a cohesive material with uniform compressive strength (UCS) of 75 kPa corresponding to a CBR (California Bearing Ratio) of 3%. A small friction and dilation angles of 1° were used for numerical stability. All material properties are defined in Table 1.

Table 1. Material properties for the Finite Element models: plate model/ railway model.

Property	Ballast	Subgrade	Plate	Geocell	Geotextile	Rail	Sleepers
ρ (kg/m^3)	1500 /1500	2162 /2162	7700 /NA*	950 /950	950 /950	NA /7852	NA /2000
E (MPa)	30 /30	8.5 /8.5	20,000 /NA	11,000 /NA	380 /380	NA /200,000	NA /30,000
φ (degrees)	45 /45	1/1	–	–	–	–	–
ψ (degrees)	10 /15	1/1	–	–	–	–	–
υ (-)	0.4 /0.4	0.35 /0.35	0.3 /NA	0.35/0.35	0.35 /0.35	NA /0.3	NA /0.25

Diamond-shaped geocells with cell width, length and height of 320 mm, 287 mm, 150 mm was used similar to the experiments discussed earlier. The geocells were modelled as an elastic material as strain levels in geocells were reported to be low with no damage in geocells were detected in the experiments (Satyal et al. 2018). The plate was modelled as a rigid body with a reference point defined at the plate centre. To reduce the computational time and taking advantage of the symmetric geometry and boundary conditions, only a quarter of the experimental box was modelled. The vertical boundaries of the ZX planes were constrained in the Y-direction, similarly, the parallel ZY planes were constrained from any lateral displacement in the X-direction. The base of the model was constrained in all three directions. The interface between the ballast and plate was modelled as hard contact in the normal direction whereas tangential slip was controlled using the Coulomb friction law with a friction coefficient of 0.4. The geocells were embedded in the ballast such that the interface friction angle between the geocell and ballast were equal to the ballast friction angle. The ballast, subgrade, loading plate and geocells were meshed using solid brick reduced integration. C3D8R elements with 9016 elements in the whole soil domain. Although some previous research used membrane elements to discretise the geocells, the differences between the membrane and solid brick elements were found to be minor. All material properties used are summarised in Table 1. Loading was applied in two steps, initially, the gravity was applied to simulate the insitu geostatic conditions. Cyclic loading of 10 kPa was applied for the first 1000 cycles, doubling every thousand cycles to a maximum of 60 kPa at 6000 loading cycles. Loading frequency of 1 Hz was used where the loading amplitude was varied using a haversine amplitude function as in the experiments. The explicit FE method is only conditionally stable and usually very small-time increments are required for accuracy (Ullah et al. 2020). Following Satyal et al. (2018), a semi-automatic mass scaling procedure with a target time increment of 0.01 seconds in the gravity step and 0.025 seconds in the following loading steps were used to reduce the computational time. Both reinforced and unreinforced models were modelled with the same geometry, materials, and boundary conditions, with and without geocells, respectively.

2.2.1 *Model validation*

The unreinforced and reinforced model data results obtained from the numerical model developed in this study were compared to the results of the experiments as well as independently conducted FE modelling data of Satyal et al. (2018), for both the geocell reinforced and unreinforced cases. Figure 3 shows the vertical settlement results with cyclic loading, with and without geocells, respectively. The results are compared at the actuator location (i.e., at plate level) and at the subgrade centre shown as solid and broken lines, respectively. The overall trend of the experiments is captured well by the numerical model. For the reinforced case, at the actuator position, good agreement is obtained between this study and the experiments up to about 4000 cycles. Beyond this the test data rises sharply to a settlement value of 90 mm compared to 80 mm predicted by the current FE model at 6000 loading cycles. The Satyal et al. (2018)

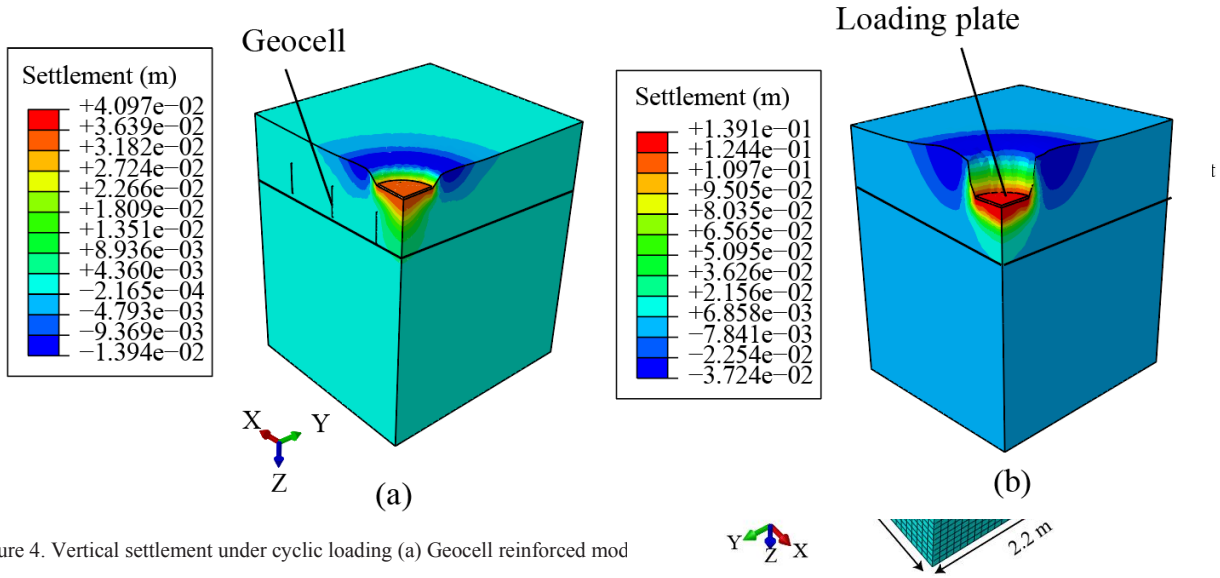

Figure 4. Vertical settlement under cyclic loading (a) Geocell reinforced mod

FE data follows closely the current FE model results with an overprediction of 7.5% at 6000 cycles. At the subgrade centre, both FE results closely match at the end of 6000 cycles with some differences over the range of 2000-4000 cycles. Both FE data matches closely the experimental values up to 3000 cycles beyond which the FE results overpredict the subgrade settlement.

For the corresponding unreinforced case, the current FE results overpredict the experiments at loading cycles > 2000 with a maximum difference of 25 % at the actuator position and 44 % at subgrade centre at 80,000 cycles. The predictions are reasonably well at the subgrade centre up to loading cycles of 3000, beyond which the current FE results overpredicts the experimental value. Figure 4 shows the vertical deformation contours at the end of 6000 loading cycles showing substantial reduction of settlement under cyclic loading for the geocell reinforced case compared to the unreinforced case.

Geocell tensile strains are an important material performance indicator. Figure 5 shows the tensile strains developed within the geocells. The maximum tensile strains were concentrated in the cells directly beneath the loading plate and the magnitude reduced in cells further away from the loading plate. The magnitudes are relatively small suggesting little damage to the geocells. These observations are consistent with post laboratory exhumed geocell condition reported in Satyal et al. (2018) which recorded no wall damage.

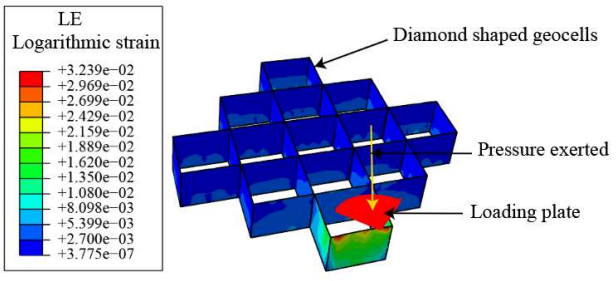

Figure 5. Tensile strain within the geocells in the geocell reinforced plate model.

2.3 *Railway FE model*

A typical railway substructure geometry provided in Australian Railway Track Cooperation (ARTC, 2012) formed the basis of the numerical railway model geometry. The embankment was 0.415 m in height, 2.2 m in width, and the ballast height was 0.3 m (height underneath the sleepers) overlying a weak subgrade. The slope of the ballast was 1:1.5 making an angle of 33 degrees with the horizontal. In the reinforced railway model, the diamond-shaped geocells were placed at 0.15 m below the bottom of the sleepers. This depth keeps the geocells safe from potential construction damage and away from direct axle loads, thus avoiding wheel load induced damage within the geocells. The geometry of the steel rail used in the simulation was a 60 kg broad gauge that is used in heavy and fast train tracks in Australia (RISSB, 2013).

Figure 6. Finite Element (FE) model of the railway structure

2.3.1 *Material properties*

The sleepers were made of concrete and were spaced at 0.5 m center to center. The geotextile and the geocells were modelled as elastic materials as strains were expected to remain within the elastic range. The elastic modulus of geotextile and geocells were estimated from the stress-strain curve corresponding to a 2% strain (Yang, 2010). The geometry of the geocells corresponded to Geoweb Australia GW30V, with a cell size of 259 by 224 mm and depth of 100 mm. Taking advantage of the symmetry only half of the railway model was modelled. All material properties used are summarised in Table 1. The Z direction and the sleeper planes along the symmetric plane were restrained in the X direction. The boundary conditions were such that along the symmetric plane the model was restrained in the X direction, The planes parallel to XZ were restrained to move in X and Y direction. The rail was allowed to move only in the vertical Z direction.

After several initial mesh trials, the ballast was meshed with linear tetrahedron C3D4 elements with a total of 11359 elements and the remaining parts including the rail, sleepers, geocells, geotextile and subgrade were meshed with linear hexahedron C3D8R elements. The total number of elements in the subgrade was 11,360. The simulations were conducted for 80,000 load cycles. The FE model is shown in Figure 6. Both with and without geocell cases were modelled for comparison.

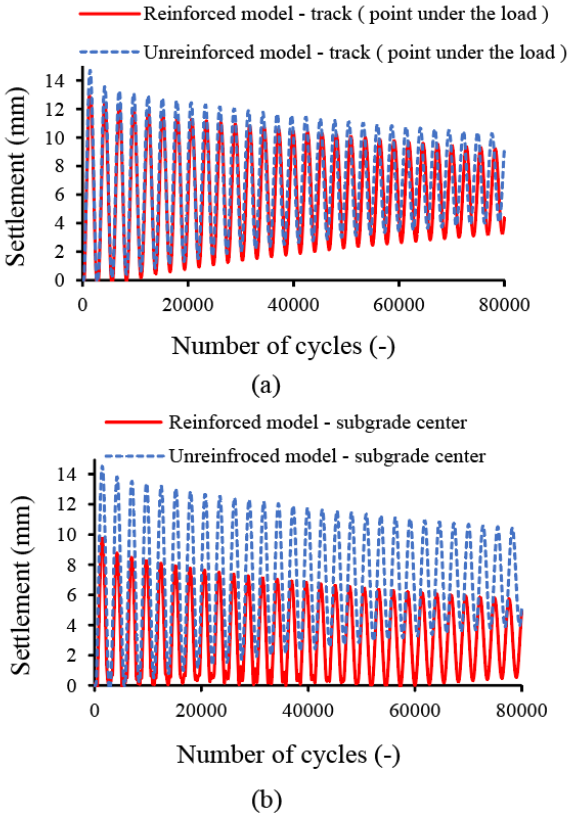

Figure 7. (a) Settlement at track level and (b) settlement at the subgrade center in a fast-moving train with and without geocells.

2.3.2 *Cyclic loading*

Loading steps were identical to that of the plate model discussed previously. The wheel load of 273 kN (considering a dynamic amplification factor of 1.4) was simulated over a small surface (0.0058 mm x 0.014 mm) on the railhead, mimicking the effect of a real-life train passing scenario. The loading was varied following a haversine function, with a loading frequency of f =16 Hz, corresponding to a train speed of 120 km/h.

2.3.3 *Results and discussions*

Figure 7 compares the track and subgrade settlement with and without geocells. The numerical model captures the unloading and reloading cycles with a reduction of track settlement for the reinforced case showing the beneficial effect of geocells. The reduction is more pronounced at the subgrade where a reduction of 45 % is noted at 80,000 cycles.

Figure 8 shows the vertical compressive stresses at the track and subgrade centre positions. It can be observed that the unreinforced model shows large stresses at the track level up to a maximum of 280 kPa. For the reinforced case, the stresses are significantly lower reaching a maximum of 150 kPa i.e., about 40% lower compared to the unreinforced case. Geocell confinement provided a more consistent distribution of subgrade stresses (Figure 8).

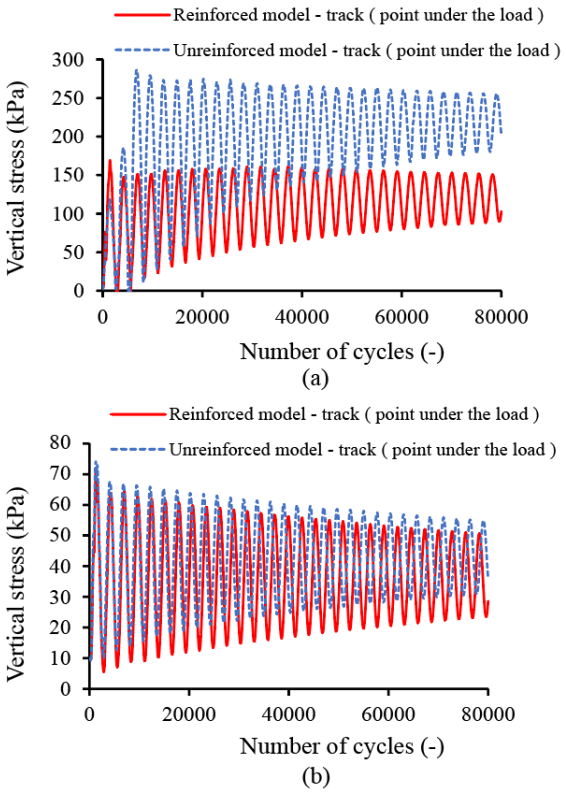

Figure 8. (a) Vertical stress at track level and (b) at subgrade center in a fast- moving train with and without geocells.

3 CONCLUSIONS

Three-dimensional FE modelling using ABAQUS/Explicit was performed for a railway built on poor quality subgrade. The effect of geocell reinforcement was studied on a standard ARTC track geometry for up to 80,000-wheel loading cycles. The train speed considered was 120 km/hr. with a loading frequency of 16 Hz. Cyclic loading experimental data was used to verify the developed model. The verification of the calibrated numerical model using finite element analysis demonstrated reasonable agreement with the data from the experimental model and proved that the geocell confinement improves the performance of the track. The following conclusions are drawn:

- Track and subgrade settlements are reduced by using geocell reinforcement. The reduction was 12% and 45% for the track and subgrade centre, respectively. The geocells reduce the unloading-reloading response fluctuations and results in a more uniform distribution of subgrade stresses.
- The vertical track stresses are substantially reduced in a geocell model compared to the no geocell case. A maximum reduction of 40% was achieved after 80000 cycles with a more uniform stress distribution for the geocell reinforced model.
- Geocell strains are mostly within the elastic range hence geocell damage is not of concern in the applications considered. Most strain concentration takes place directly beneath the load.
- The improvements reported are valid for relatively poor-quality ballast overlying soft clay of CBR of 3%. Future parametric studies are planned for a more detailed study on ballast quality and subgrade strength.

4 ACKNOWLEDGEMENTS

The first author acknowledges her research scholarship provided under the Women in Engineering Scholarship scheme at the Central Queensland University. The authors acknowledge the discussions with Prof. Buddhima Indraratna from the University Technology Sydney and A/Prof. Ben Leshchinsky from Oregon State University in clarifying their research on the topic. Thanks are due to Mr. Daniel Gibbs from Geofabrics Australia for providing valuable technical information and research insight on geocells during the early stages of this work. All simulations are conducted using CQ University High-Performance Computing facilities. These supports are gratefully acknowledged.

5 REFERENCES

ABAQUS. ABAQUS analysis user's manual. Version 2019: Dassault Systemes Simulia Corp: 2019.

Ahlf, R. E. (1975). M/W Costs: How they are affected by car weights and the track structure. *Railway track and structures, 71*(3).

ARTC (2012). Australian Rail Track Corporation LTD, Engineerin g, Ballast section 4 (Track &Civil), Code of practice, (201 2).

behavior of railway ballasted structure with geocell conf ine ment.(Report). Geotextiles and Geomembrans 36, 33.

Biabani, M. M., Indraratna, B., & Ngo, N. T. (2016). Modelling of geocell-reinforced sub ballast subjected to cyclic loa ding. Geotextiles and Geomembranes, 44(4), 489- 503. doi:10.101 6/j.geotexmem.2016.02.001

Biswas, A., & Krishna, A. (2017). Geocell-Reinforced Foundation Systems: A Critical Review. International Jour. nal of Geosynthetics and Ground Engineering, 3(2), 1-18. doi: 10.1007/s40891-017-0093-7

Dash, S. K., Krishnaswamy, N., & Rajagopal, K. (2001). Bearing capacity of strip footings supported on geocell-reinforce d s and. Geotextiles and Geomembranes, 19(4), 235-256.

Dash, S. K., Krishnaswamy, N., & Rajagopal, K. (2001). Bearing capacity of strip footings supported on geocell-reinforced sand. *Geotextiles and Geomembranes, 19*(4), 235-256.

Dash, S., & Shivadas, A. (2012). Performance Improvement of Railway Ballast Using Geocells. *Indian Geotechnical Journal, 42*. doi:10.1007/s40098-012-0017-3

Garcia, R. S., & Avesani Neto, J. O. (2021). Stress-dependent me thod for calculating the modulus improvement factor in g. e ocell-reinforced soil layers. Geotextile s and Geo membranes 49(1), 146- 1 58. doi: 10.1016/j.geot exmem.2020.09.009.

Hegde, A. (2017). Geocell reinforced foundation beds-past findings, present trends and future prospects: A state-of-the-art review. *Construction and Building Materials, 154*, 658-674. doi:10.1016/j.conbuildmat.2017.07.230

Hegde, A., & Sitharam, T. G. (2013). Experimental and numerical studies on footings supported on geocell reinforced sand and clay beds. *International Journal of Geotechnical Engineering, 7*(4), 346-354. doi:10.1179/1938636213Z.00000000043

Indraratna, B. (2008). Recent advancements in the use of prefabric ated vertical drains in soft soils. UoW, Faculty of Engi neer ing-papers, https://ro.uow.edu.au/engpapers/418.

Indraratna, B., & Nimbalkar, S. (2013). Stress-strain degradation response of railway ballast stabilised with geosynthetics. *Journal of Geotechnical and Geoenvironmental Engineering, 139*(5), 684-700.

Indraratna, B., Biabani, M. M., & Nimbalkar, S. (2015). Behaviour of geocell-reinforced sub-ballast subjected to cyclic loading in plane-strain condition. *Journal of Geotechnical and Geoenvironmental Engineering, 141*(1), 04014081.

Indraratna, B., Sun, Q., Ngo, T., & Rujikiatkamjorn, C. (2017). Current research into ballasted rail tracks: model tests and their practical implications. *Australian Journal of Structural Engineering, 18*, 1-17. doi:10.1080/13287982.2017.1359398

Keeng, N., Li, J., & Hao, H. (2015). Effect of High-Speed Rail Transit and Impact Loads on Ballast Degradation. In (Vol. 19, pp. 521-531).

Lackenby, J., Indraratna, B., McDowell, G., & Christie, D. (2007). Effect of confining pressure on ballast degradation and deformation under cyclic triaxial loading. *Géotechnique, 57*(6), 527-536. doi:10.1680/geot.2007.57.6.527

Leshchinsky, B., & Ling, H. I. (2013). Numerical modelling of behaviour of railway ballasted structure with geocell confinement. *Geotextiles and Geomembranes, 36*(C), 33-43. doi:10.1016/j.geotexmem.2012.10.006

Mhaiskar, S. Y., & Mandal, J. N. (1996). Investigations on soft clay subgrade strengthening using geocells. *Construction and Building Materials, 10*(4), 281-286. doi:10.1016/0950-0618(95)00083-6

Murali Krishna, A., & Biswas, A. (2017). *GEOCELL REINFORCED FOUNDATIONS*.

Nimbalkar, S., Neville, T., & Indraratna, B. (2014). Performance assessment of reinforced ballasted rail track. *Proceedings of the ICE - Ground Improvement, 167*, 24-34. doi:10.1680/grim.13.00018

Qian, Y., Han, J., Pokharel, S. K., & Parsons, R. L. (2010). Experimental study on triaxial geogrid-reinforced bases over weak subgrade under cyclic loading. In *GeoFlorida 2010: Advances in Analysis, Modeling & Design* (pp. 1208-1216).

Rajagopal, K., Krishnaswamy, N. R., & Madhavi Latha, G. (1999). Behaviour of sand confined with single and multiple geocells. *Geotextiles and Geomembranes, 17*(3), 171-184. doi:10.1016/S0266-1144(98)00034-X

RISSB (2013). Rail track material, Part 1: Steel rails, AS 1085.1: 2013.

Satyal, S. R., Leshchinsky, B., Han, J., & Neupane, M. (2018). Use of cellular confinement for improved railway performance on soft subgrades. *Geotextiles and Geomembranes, 46*(2), 190-205.

Selig, E. T., & Waters, J. M. (1994). *TRACK GEOTECHNOLOGY and SUBSTRUCTURE MANAGEMENT*: Thomas Telford Publishing.

Skempton, A. (1951). The bearing capacity of clays. *Selected Papers on Soil Mechanics*, 50-59.

T.K.Dam, L., Sandanbata, I., Kimura., M (2006): Vacuum Consolidation method – Worldwide Practice and the Lastest Improvement in Japan, Technical Research Report of Hazama Corporation, ISSN:1880-2370, Vol. 38.
(PDF) Vacuum Preloading Consolidation Method, A Case Study of Dinh Vu Polyester Plant, pp 1-16.

Ullah, S. N., Noor-E-Khuda, S., Lee, F.-H., Suntharavadivel, T., & Albermani, F. (2020). Deep Undrained Bearing Capacity of Rectangular Foundations in Uniform Strength Clay. Journal of Geotechnical and Geoenvironme ntal Engineering, 146. D oi:10.1061/%28ASCE%2 9GT.1943-5606.0002356

Webster, S. L., & Alford, S. J. (1978). *Investigation of constructionconcepts for pavements across soft ground* (Vol. 78): US Army Engineer Waterways Experiment Station.

Yang, X., Han, J., Parsons, R. L., & Leshchinsky, D. (2010). Thr ee-dimensional numerical modelling of single geocell-rei n forced sand. *Frontiers of Architecture and Ci vil Engineer ng in China, 4*(2), 233-240.